

# Study of Electromigration in Eutectic SnPb Solder Stripes Using the Edge Displacement Method

C.K. CHOU,<sup>1</sup> Y.C. HSU,<sup>1</sup> and CHIH CHEN<sup>1,2</sup>

1.—Department of Material Science and Engineering, National Chiao Tung University, Hsin-chu 30050, Taiwan, Republic of China. 2.—E-mail: chih@cc.nctu.edu.tw

Electromigration (EM) parameters in the eutectic SnPb solder were measured using the edge displacement method (EDM) and an atomic force microscope (AFM) in the temperature range of 60° to 140°C. The measured drift velocity was found to be 0.3 Å/sec when the solder stripe was stressed under  $4.9 \times 10^4$  A/cm<sup>2</sup> at 80°C, and it increased as the current density or the temperature increased. The products of  $DZ^*$  at 60°C, 80°C, 100°C, 120°C, and 140°C were also obtained. In addition, the EM activation energy was determined to be 0.45 eV at the temperature range 60–100°C and 0.55 eV at the temperature range 100–140°C. These two activation energies may correspond to the Sn and Pb diffusion at the two temperature ranges. These values are very fundamental to current-carrying capability and mean-time-to-failure measurement for solder joints.

**Key words:** Electromigration (EM), flip-chip solder, packaging

## INTRODUCTION

Flip-chip technology has become an important integrated circuit (IC) packaging method. One of its advantages is that a large number of tiny solder bumps can be fabricated into an area array on a chip as input/output (I/O) interconnections. To meet the increasing performance requirements, the I/O number keeps increasing. Thus, the size of the bumps shrinks continuously, causing rapid increase in the current density passing through each bump. The size of these solder bumps is quite small, with a diameter of about 100 μm or less. The design rule for packaging requires that each bump carries 0.2–0.4 A. The current density may reach  $5\text{--}10 \times 10^3$  A/cm<sup>2</sup>. Therefore, electromigration (EM) has become an important reliability issue for flip-chip joints.<sup>1,2</sup>

Eutectic SnPb solder has been implemented in flip-chip technology for decades due to its low melting point and excellent mechanical properties.<sup>3–5</sup> Therefore, the use of the SnPb solder will continue until the year of 2010. However, EM will be a limiting factor for application of the SnPb solder to high-performance devices. Since the SnPb solder is a binary alloy, the diffusion behavior during EM is more complicated than that in Al or Cu.<sup>1</sup> Several studies have investigated the EM behavior in the SnPb alloy.<sup>6–10</sup> Liu et al. found that the dominant

diffusion species was Sn atoms in a thin SnPb stripe when stressed at room temperature.<sup>6</sup> Huynh conducted another EM study at 150°C using V-groove samples and found that Pb atoms were the dominant diffusion species.<sup>7</sup> This is because Pb atoms have higher diffusivity than Sn atoms above 151°C.<sup>11</sup>

In general, the atomic flux of EM “ $J_{EM}$ ” in a conductor driven by a constant current density “ $j$ ” can be expressed as follows:<sup>12</sup>

$$J_{EM} = CDZ^* eE = C \left( \frac{D_0}{kT} \right) \exp \left( - \frac{E_a}{kT} \right) Z^* e \rho j \quad (1)$$

where  $J_{EM}$  is the EM flux,  $C$  is the concentration of atoms per unit volume of the eutectic alloy,  $D$  is the effective lattice diffusivity of the solder at testing temperature,  $Z^*$  is the effective charge number,  $E$  is the electric field,  $D_0$  is the prefactor for the diffusivity,  $E_a$  is the activation energy for EM,  $\rho$  is resistivity of the film,  $k$  is the Boltzmann’s constant, and  $T$  is the absolute temperature. Among these factors,  $Z^*$  is the most important parameter of EM. The product of  $DZ^*$  for an eutectic SnPb solder was found to be  $-3.3 \times 10^{-8}$  cm<sup>2</sup>/s for a fixed length of V-groove solder lines stressed by  $2.8 \times 10^4$  A/cm<sup>2</sup> at 150°C,<sup>7</sup> and it was  $-1.85 \times 10^{-10}$  cm<sup>2</sup>/s when measured by the marker movement in solder bumps stressed by  $1.0 \times 10^4$  A/cm<sup>2</sup> at 120°C. However, the fundamental parameters of EM at temperature 80–120°C, such as drift velocity, activation energy ( $E_a$ ), and the product

of diffusivity and effective charge number ( $DZ^*$ ) of the eutectic SnPb solder, are still unknown.

We have developed a technique that can measure the preceding parameters using the edge displacement method.<sup>13</sup> In this paper, the drift velocities at various stressing conditions were measured at the temperature range of 60–140°C. The fundamental EM parameters can be measured or estimated. Thus, this study provides more fundamental understanding on the EM behavior in eutectic SnPb alloy.

## EXPERIMENTAL

Eutectic SnPb solder stripes were fabricated in Si trenches of 3.1- $\mu\text{m}$  depth. The fabrication procedure was described in detail in our previous publication.<sup>13</sup> Fig. 1a and b shows the cross-sectional and the plan-view schematics, respectively, for the SnPb solder stripe in the Si trench. The dimension of the solder stripe was 80- $\mu\text{m}$  wide, 370- $\mu\text{m}$  long, and 3.1- $\mu\text{m}$  thick. A copper layer of 0.4  $\mu\text{m}$  was used as a wetting layer. The intermetallic compound (IMC) of  $\text{Cu}_6\text{Sn}_5$  was formed after the reflow at 210°C for 4 sec on a hot plate. A desired current was applied through the two pads on a hot plate of a probe station. The test structure is also known as the Blech specimen.<sup>14</sup> An atomic force microscope (AFM) was used to measure the depletion volume on the cathode side of the samples. The AFM used in this study was DI Nanoscope E (Veeco Instruments, Inc., Woodbury, NY). Each specimen was scanned 6 times by the AFM to measure the volume before and after current stressing, and the standard deviation was less than 1% compared with the average volume. The increase in temperature due to Joule heating effect was monitored by an infrared microscope (Quantum Focus Instruments Corp., Vista, CA), which has 0.1°C temperature resolution and 2- $\mu\text{m}$  spatial resolution.<sup>15</sup>

Transmission electron microscopy (TEM) was employed to investigate the microstructure of the interface between the solder and the Cu layer. A focused ion beam was used to prepare cross-sectional TEM specimens. Scanning electron microscopy (SEM) and energy dispersive spectroscopy were used to examine the microstructure evolution and composition of the solder, respectively.

## RESULTS

Solder stripes with a smooth surface can be fabricated by this technique. Figure 2a shows the plan-view SEM image of a fabricated Blech specimen, and the middle solder stripe is of interest. The cross-sectional TEM image of the solder strip is shown in Fig. 2b, in which the solder,  $\text{Cu}_6\text{Sn}_5$  IMC, remaining Cu under bump metallization (UBM), and the Ti layers can be observed clearly. The average grain size was about 0.8  $\mu\text{m}$  for this sample. It is worth noting that there was no continuous Cu layer left after the sample fabrication process, which is beneficial to the current study. Otherwise, there will be a large fraction of the applied current flowing in the Cu layer, since Cu has a very low resistivity of 1.7  $\mu\Omega\text{-cm}$ . The average thickness of the IMC layer was 0.6  $\mu\text{m}$ , with approximately 80% of the applied current drifting in the solder stripe, 19% in the IMC layer, and only 1% in the Ti layer. The increase in temperature due to the Joule heating effect as a function of applied current was shown in Fig. 3. The temperature increase due to the Joule heating rose with increasing applied current. However, the maximum temperature was only 1.8°C for the most severe stressing condition in this study. This may be due to the large area for heat dissipation and the excellent heat conduction in the Si substrate. Therefore, the Joule heating effect was not serious in the solder Blech specimen.

Figure 4a shows the plan-view SEM image of a fabricated solder stripe, and its corresponding AFM image was shown in Fig. 4b. The AFM was capable of measuring the profile of the solder stripe. After it was stressed by  $3 \times 10^4 \text{ A/cm}^2$  at 100°C for 72 h, depletion occurred in the cathode end of the stripe, as shown in Fig. 4c. The corresponding AFM image was illustrated in Fig. 4d. The depletion volume can be estimated from Fig. 4b and d using an in-house computer program. Thus, drift velocity can be calculated.

The EM rate near the device operation temperature of 100°C is of interest, because voids form after the depletion of the solder near the cathode end. Figure 5 shows the measured drift velocity as a function of applied current density at 80°C, 100°C, and 120°C. The drift velocity was measured to be 0.3  $\text{\AA}/\text{sec}$  under  $4.9 \times 10^4 \text{ A/cm}^2$  at 80°C, and it

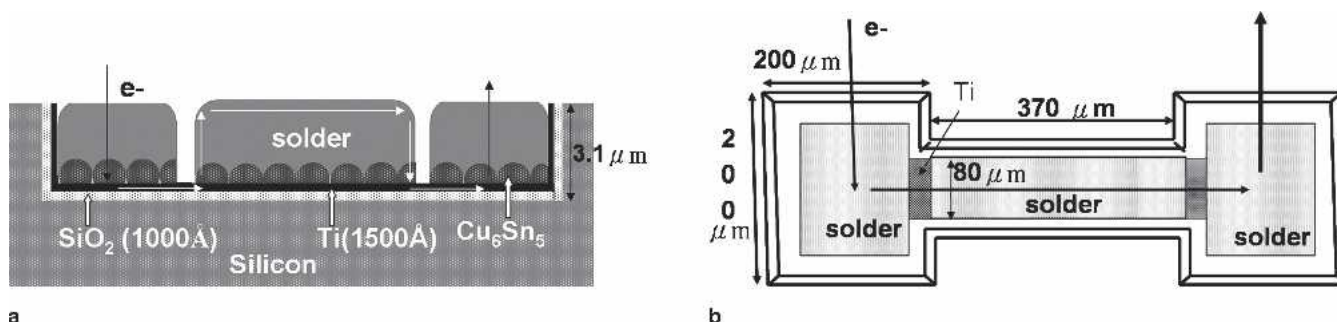
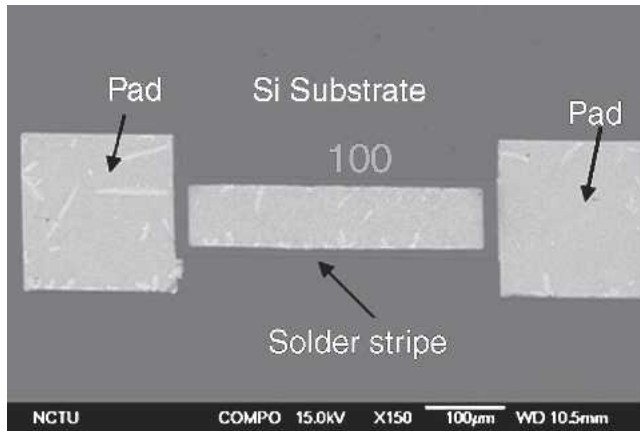
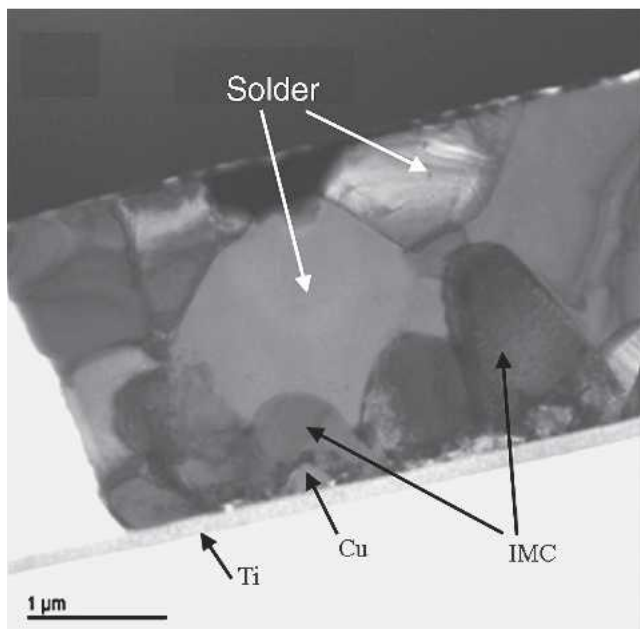


Fig. 1. The schematics of solder Blech specimens. (a) Cross-sectional diagram of a solder strip inside the Si trench. (b) Plan-view diagram of the solder strip on the Cu/Ti metallization layer. The SnPb strip was 370- $\mu\text{m}$  long, 80- $\mu\text{m}$  wide, and approximately 3.1- $\mu\text{m}$  thick.



a



b

Fig. 2. SEM images for a fabricated Blech specimen. (a) Plan-view image, in which the SnPb solder stripe and the two pads are labeled. (b) Cross-sectional TEM image of a solder strip. The average thickness of the IMC layer is 0.6 µm.

increased as the current density or the temperature increased. It was as high as 5.3 Å/sec under  $1.1 \times 10^5$  A/cm<sup>2</sup> at 120°C. It increases when the applied current or the temperature increases. At 100°C, the velocity increased from 0.4 Å/sec under  $3.0 \times 10^4$  A/cm<sup>2</sup> to 1.4 Å/sec under  $1.0 \times 10^5$  A/cm<sup>2</sup>.

To measure more precisely the activation energy, the drift velocity was measured at 60°C and 140°C. The average drift velocity (V) due to EM is given by Huntington and Grone:<sup>12</sup>

$$V = \frac{J}{C} = BeZ * \rho j = \left( \frac{D_0}{kT} \right) eZ * \rho j \exp\left( \frac{-E_a}{kT} \right) \quad (2)$$

where J is the atom flux, C is the density of metal ions, B is the mobility, k is Boltzmann's constant, T is the absolute temperature, eZ\* is the effective charge of the ions, ρ is the metal resistivity, j is the electrical current density, E<sub>a</sub> is the activation

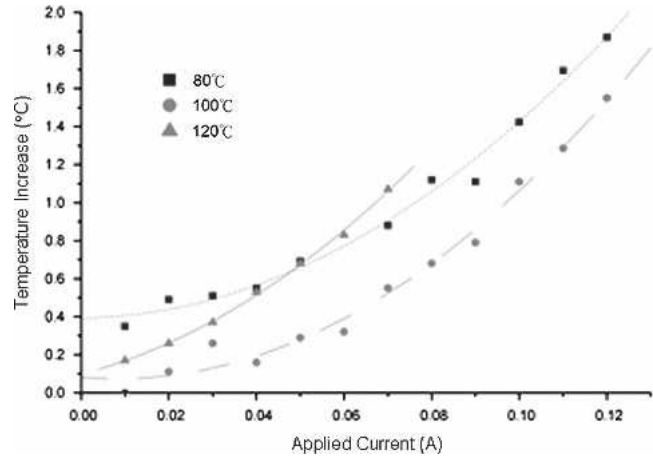
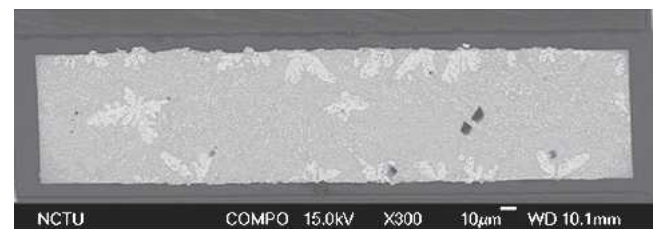


Fig. 3. The increase in measured temperature inside the solder stripe as a function of applied current at 80°C, 100°C, and 120°C.

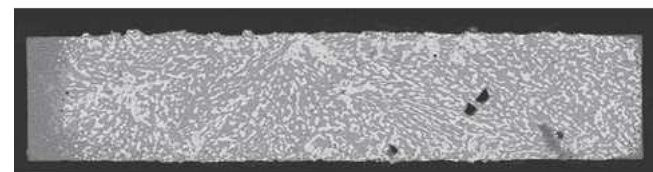
energy of diffusion, and D<sub>0</sub> is the prefactor of the diffusion constant. Equation 2 can be rewritten as

$$\frac{VT}{j} = \frac{D_0 eZ * \rho}{k} \exp\left( \frac{-E_a}{kT} \right) \quad (3)$$

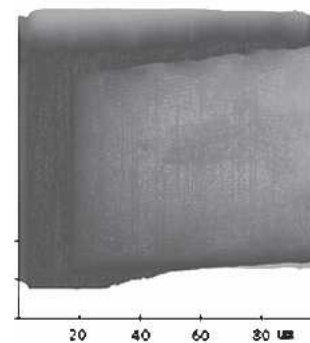
Taking the logarithm of both sides of Eq. 2 yields



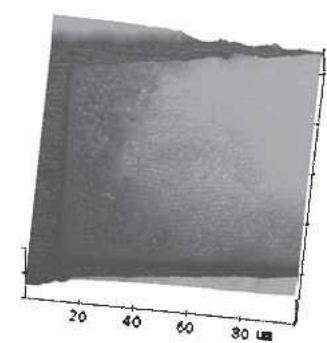
a



b



c



d

Fig. 4. (a) Plan-view back-scattered SEM image of a SnPb solder strip before current stressing, in which the brighter region represents the Pb-rich phase and the darker region corresponds to the Sn-rich phase. (b) AFM image of the cathode end for the solder strip in (a). (c) The solder stripe in (a) after current stressing of  $3 \times 10^4$  A/cm<sup>2</sup> at 100°C for 72 h. (d) AFM image of the cathode end for the solder strip in (b).

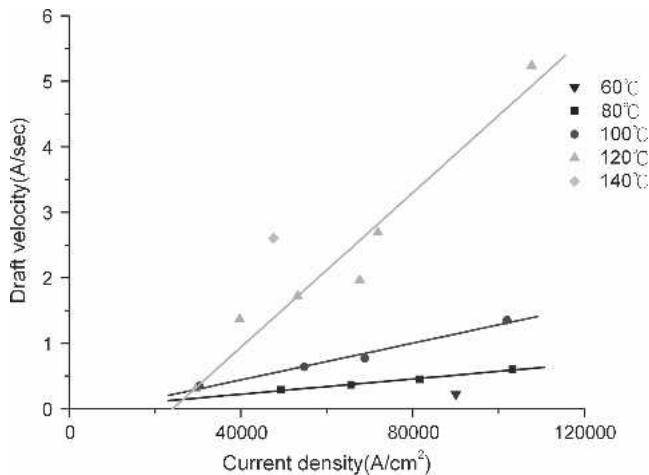


Fig. 5. The average drift velocity of the SnPb solder as a function of applied current density at 80°C, 100°C, and 120°C. The threshold current densities were obtained by extrapolating the fitted lines to zero drift velocity.

$$\ln \frac{VT}{j} = -\left(\frac{E_a}{kT}\right) + \ln \frac{D_0 e Z^* \rho}{k} \quad (4)$$

Therefore, by measuring the drift velocity as a function of reciprocal temperature, the activation energy  $E_a$  and the product of diffusivity and effective charge number  $DZ^*$  can be obtained. Table I lists the measured  $DZ^*$  at various temperatures. The value ranged from  $4.88 \times 10^{-11} \text{ cm}^2/\text{s}$  at 60°C to  $1.34 \times 10^{-9} \text{ cm}^2/\text{s}$  at 140°C. Figure 6 shows the plot of  $\ln(vT/j)$  as a function of the reciprocal temperature. Surprisingly, two slopes were found in the plot, and the turning point occurred at about 100°C. The calculated activation energy was 0.45 eV at the temperature range 60–100°C and 0.55 eV at the temperature range 100–140°C.

The microstructure in the anode side varied with the stressing temperature. Figure 7a shows the backscattering SEM image for the hillocks formed at the anode side of the solder stripe after the current stressing of  $8.0 \times 10^4 \text{ A/cm}^2$  at 80°C for 72.0 h. It is found that Sn atoms were the dominant diffusion species, since they pushed the Pb-rich grain up, as shown in the enlarged image in Fig. 7b. These results agree with the ones obtained at room temperature.<sup>7</sup> When stressed by  $6.9 \times 10^4 \text{ A/cm}^2$  at 100°C for 34.7 h, no obvious dominant diffusion

**Table I. Values for the Product of the Diffusivity and the Effective Charge Number at Various Temperatures**

Temperature	Measured $DZ^*$ ( $\text{cm}^2/\text{sec}$ )	Calculated $Z^*$
60°C	$4.88 \times 10^{-11}$	0.068
80°C	$1.19 \times 10^{-10}$	0.029
100°C	$2.64 \times 10^{-10}$	0.014
120°C	$7.48 \times 10^{-10}$	0.090
140°C	$1.34 \times 10^{-9}$	0.051

species could be differentiated, as illustrated in Fig. 7c and d. It is speculated that the fluxes of Sn and Pb atoms are approximately at the same order. Nevertheless, Pb atoms seemed to be the dominant species when stressed at 120°C. Figure 7e shows the SEM image for the hillocks grown on the anode of the solder stripe stressed by  $5.3 \times 10^4 \text{ A/cm}^2$  at 120°C for 20.8 h, and the enlarged image for the hillocks is illustrated in Fig. 7f. A large amount of Pb atoms accumulated at the bottom of the large hillock in the figure, which agrees with the results obtained at 150°C, as reported by Huynh et al.

## DISCUSSION

In our previous publication, we assumed that the relationship between the drift velocity and the applied current density behaves linearly and used the extrapolation method to obtain the threshold current density.<sup>13</sup> However, due to the existence of back stress,<sup>16,17</sup> the relationship may not be linear. In addition, Pb-rich and Sn rich phases redistribute during EM, which makes the stress issue more complicated. Therefore, the use of extrapolation in SnPb solder stripes may be problematic.

The difference in dominant diffusion species may be responsible for the opposite trend of the temperature dependence of the threshold current density and the two slopes in the plot of  $\ln(vT/j)$  as a function of the reciprocal temperature. As shown in Fig. 7a through f, the dominant diffusion species were Sn at 60°C and below, whereas they were Pb at 120°C and above. Therefore, it is inferred that the measured activation energy of 0.45 eV from 60°C to 100°C corresponds to the Sn diffusion, and the 0.55 eV from 100°C to 140°C corresponds to the Pb diffusion. For the threshold current density, Pb atoms were the dominant species at 120°C, which may be responsible for the higher  $J_c$  value, since Pb atoms have a higher melting point.

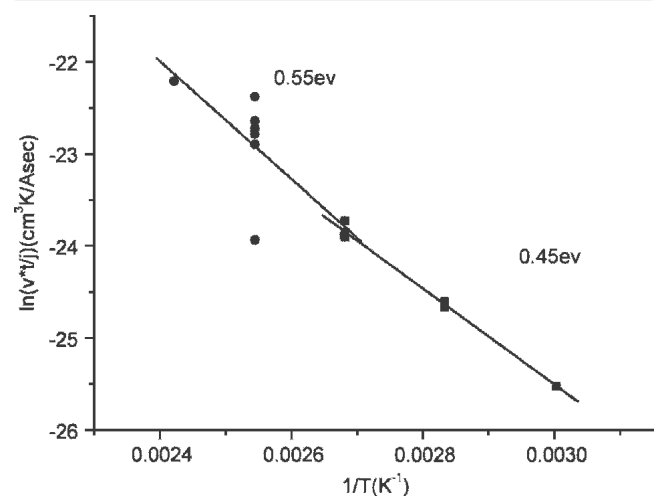


Fig. 6. The plot of the  $\ln(vT/j)$  as a function of reciprocal temperature. The activation energy was determined to be 0.45 eV below 100°C and 0.60 eV above 100°C.

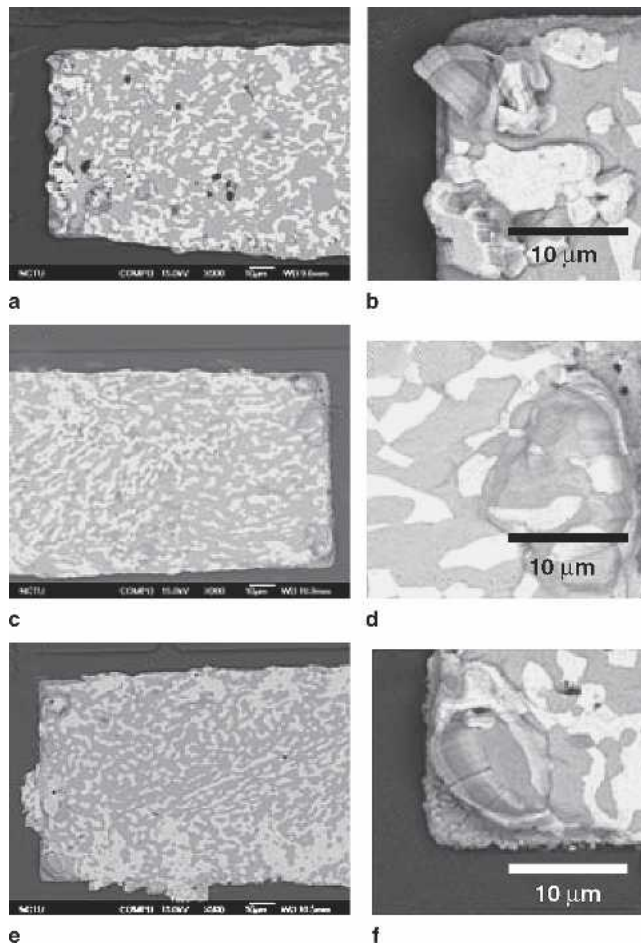


Fig. 7. Backscattered SEM images for the hillocks formed at the anode side of the solder stripe: (a) after current stressing of  $8.0 \times 10^4$  A/cm<sup>2</sup> at 80°C for 72.0 h, (b) enlarged image of (a), (c) after current stressing of  $6.9 \times 10^4$  A/cm<sup>2</sup> at 100°C for 34.7 h, (d) enlarged image of (c), (e) after current stressing of  $5.3 \times 10^4$  A/cm<sup>2</sup> at 120°C for 20.8 h, and (f) enlarged image of (e).

## CONCLUSIONS

The EM parameters for the eutectic SnPb solder have been measured using the Blech specimen and an AFM in the temperature range of 60°C to 140°C. The drift velocity was measured at various current densities. The product of  $DZ^*$  was measured to be  $4.88 \times 10^{-11}$  cm<sup>2</sup>/sec,  $1.19 \times 10^{-10}$  cm<sup>2</sup>/sec,  $2.64 \times 10^{-10}$  cm<sup>2</sup>/sec,  $7.48 \times 10^{-10}$  cm<sup>2</sup>/sec, and  $1.34 \times 10^{-9}$  cm<sup>2</sup>/sec at 60°C, 80°C, 100°C, 120°C, and 140°C, respectively. In addition, the EM activation energy was measured to be 0.45 eV below 100°C and 0.55 eV above 100°C. Different dominant diffusion species may be responsible for the two activation energies.

## REFERENCES

1. K.N. Tu, *J. Appl. Phys.* 94, 5451 (2003).
2. *The International Technology Roadmap for Semiconductor* (2003).
3. K.N. Tu and K. Zeng, *Mater. Sci. Eng., R* R34, 1 (2001).
4. L.F. Miller, *IBM J. Res. Development* 13, 239 (1969).
5. P.A. Totta and R.P. Sopher, *IBM J. Res. Development* 13, 226 (1969).
6. S. Brandenburg and S. Yeh, *Proc. Surface Mount Int. Conf. Exhib., SM198* (Edina, MN: SMTA, 1998), p. 337.
7. C.Y. Liu, C. Chen, and K.N. Tu, *J. Appl. Phys.* 88, 5703 (2000).
8. Q.T. Huynh, C.Y. Liu, C. Chen, and K.N. Tu, *J. Appl. Phys.* 89, 4332 (2001).
9. T.Y. Lee, K.N. Tu, S.M. Kuo, and D.R. Frear, *J. Appl. Phys.* 89, 3189 (2001).
10. H. Ye, C. Basaran, and D. Hopkins, *Appl. Phys. Lett.* 82, 7 (2003).
11. D. Gupta, K. Vieregge, and W. Gust, *Acta Mater.* 47, 5 (1999).
12. H.B. Huntington and A.R. Grone, *J. Phys. Chem. Solids* 20, 76 (1961).
13. Y.T. Yeh, C.K. Chou, Y.C. Hsu, and K.N. Tu, *Appl. Phys. Lett.* 86, 203504 (2005).
14. I.A. Blech, *J. Appl. Phys.* 47, 1203 (1976).
15. T.L. Shao, S.H. Chiu, D.J.C. Chen, X. Yao, and C.Y. Hsu, *J. Electron. Mater.* 33, 1350 (2004).
16. I.A. Blech, *Acta Mater.* 46, 3717 (1998).
17. P.C. Wang, G.S. Cargill, I.C. Noyan, and C.K. Hu, *Appl. Phys. Lett.* 72, 1296 (1998).